

Structural and Electronic Factors in Heterolytic Cleavage: Formation of the Co(I) Intermediate in the Corrinoide/Iron–Sulfur Protein from *Clostridium thermoaceticum*[†]

Michael D. Wirt,[‡] Manoj Kumar,[§] Jing-jing Wu,^{||} Eva M. Scheuring,^{||} Stephen W. Ragsdale,^{*,§,||} and Mark R. Chance^{*,||,§}

Departments of Molecular Pharmacology and Physiology and Biophysics, Albert Einstein College of Medicine of Yeshiva University, 1300 Morris Park Avenue, Bronx, New York 10461, and Department of Biochemistry, East Campus, University of Nebraska, Lincoln, Nebraska 68583-0718

Received October 24, 1994; Revised Manuscript Received January 31, 1995[®]

ABSTRACT: We have completed the first direct structural characterization of an enzyme-bound four-coordinate Co(I) intermediate, in this case for the corrinoide/iron–sulfur protein (C/Fe-SP) from *Clostridium thermoaceticum*. Extended X-ray absorption fine structure and X-ray edge spectroscopy of the active Co(I) state of the C/Fe-SP indicates a four-coordinate (distorted) square-planar structure where the best fit gives average Co–N(equatorial) distances of 1.87 ± 0.01 Å, corresponding to 4.2 ± 0.3 ligands. The X-ray edge spectrum of Co(I) C/Fe-SP contains a moderate intensity 1s-4p + “shake-down” (SD) transition and no 1s-3d peak (where SD transitions are indicative of square-planar geometries). X-ray edge results for the methyl-Co(III) form, reported earlier [Wirt, M. D., Kumar, M., Ragsdale, S. W., & Chance, M. R. (1993) *J. Am. Chem. Soc.* 115, 2146–2150], are consistent with a base-off methylcobamide structure. The absence of a ligated 5-methoxybenzimidazole base in the methyl-Co(III) state is important since the base-off form is predicted to predispose the Co–C bond toward heterolytic cleavage to form the four-coordinate Co(I) species concurrent with methyl transfer. Additionally, we have examined first-derivative X-ray edge spectra of Co(I) C/Fe-SP, relative to edge spectra of a cobalt foil, as an indicator of effective nuclear charge on cobalt. The Co(I) C/Fe-SP edge position at 7720.5 ± 0.3 eV is less than, but very close to, the value seen for the corresponding free Co(I) cobalamin. The observed reduction in effective nuclear charge for protein-bound cobamides in Co(I), Co(II), and Co(III) oxidation states may promote heterolytic Co–C bond cleavage by increasing the electrophilic nature of the donated methyl group and increase the nucleophilicity of enzyme bound Co¹⁺ to facilitate remethylation of the cofactor.

The corrinoide/iron-sulfur protein (C/Fe-SP) from *Clostridium thermoaceticum* plays an important role as a methyl carrier protein in the reductive acetyl-CoA pathway. Methyl transferase catalyzes the transfer of a methyl group from methyl tetrahydrofolate (CH₃-H₄ folate) to the C/Fe-SP to form a methyl-Co (III) species (Figure 1). This methyl group is then transferred to carbon monoxide dehydrogenase (CODH), which catalyzes the final steps in acetyl-CoA synthesis (Lu *et al.*, 1990). The C/Fe-SP cycles between a methyl-Co(III) and Co(I) form in this process. In transfer of the methyl group to CoDH, formation of the nucleophilic Co(I) intermediate is believed to proceed through heterolytic Co–C bond cleavage of the base-off Co(III) 5-methoxybenzimidazolymethylcobamide parent (Ragsdale *et al.*, 1987; Harder *et al.*, 1989; Hu *et al.*, 1984). In addition to the cobamide, a [4Fe-4S]^{2+/+} cluster has been identified in the C/Fe-SP (Ragsdale *et al.*, 1987).

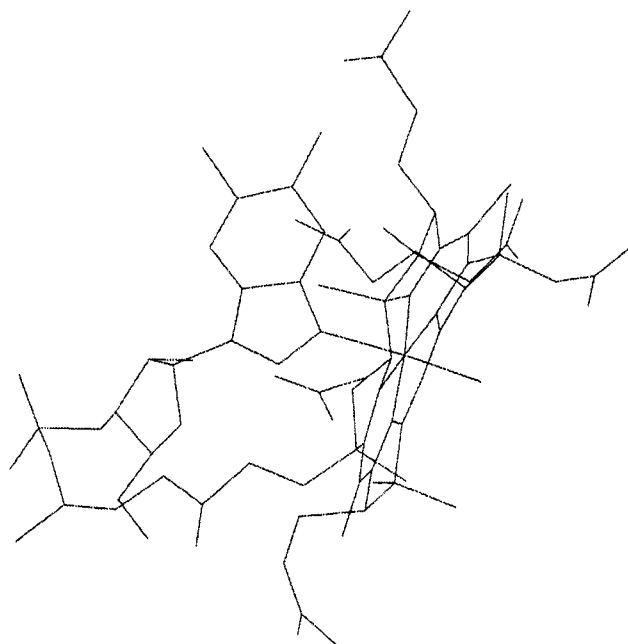


FIGURE 1: Structure of methylcobalamin (MeCbl) in a “base-on” configuration (Rossi *et al.*, 1985). The base-off form of methylcobalamin is generated by cleavage of the axial cobalt–nitrogen bond to the benzimidazole base. The MeCbl structure was obtained from the Cambridge Crystallographic Data Base version 5 (Allen *et al.*, 1983) and plotted using the Chem-X molecular modeling program.

[†] This research is supported by NRICGP/CSRS/USDA Grant 91-37200-6897 (M.R.C.) and NIH Grant RO1-GM-39451 (S.W.R.).

^{*} Authors to whom correspondence should be addressed.

[‡] Department of Molecular Pharmacology, Albert Einstein College of Medicine of Yeshiva University.

[§] University of Nebraska, Lincoln.

^{||} Department of Physiology and Biophysics, Albert Einstein College of Medicine of Yeshiva University.

[†] Phone: (402) 472-2943. Facsimile: (402) 472-7842. Bitnet: sragdale@crvms.unl.edu.

[‡] Phone: (718) 430-4136. Facsimile: (718) 430-8819. Internet: mrc@aecom.yu.edu.

[®] Abstract published in *Advance ACS Abstracts*, March 15, 1995.

Comparison of structural and electronic information collected from free cobalamins and their derivatives with data from relevant oxidation states of enzyme bound B₁₂ cofactors provides an initial starting point from which insight into the mechanisms of both heterolytic Co–C bond cleavage and methyl transfer reactions is gained. In this study, we have employed extended X-ray absorption fine structure (EXAFS) and X-ray edge spectroscopy to probe the local molecular structure of the catalytically important Co(I) state of the C/Fe-SP. Both EXAFS and X-ray edge analysis indicate a four-coordinate (distorted) square-planar structure in which the 5-methoxybenzimidazole base remains detached from cobalt. This result provides the first direct evidence for an enzyme-bound four-coordinate Co(I) C/Fe-SP species like that of free Co(I) B₁₂ (Wirt *et al.*, 1992). These results, coupled with recent methyl-Co(III) and Co(II) C/Fe-SP data (Wirt *et al.*, 1993a), demonstrate that a base-off configuration is maintained for all three cobamide oxidation states. Additionally, we have found a consistent shift in the effective nuclear charge on cobalt to lower energy for the enzyme-bound cobamide cofactor when compared with analogous free cobalamins. Examination of the electronic and structural characteristics of the Co(I), Co(II), and Co(III) series for C/Fe-SP furnishes convincing evidence for protein-mediated modification of the cobamide to facilitate the heterolytically generated transfer of a methyl group to CODH. In addition, this is apparently the first structural characterization of a Co(I) enzyme state.

MATERIALS AND METHODS

Materials. Aluminum oxide and 5,10,15,20-tetraphenyl-21*H*,23*H*-porphine cobalt(II) (CoTPP) were purchased from Aldrich Chemical Co. and were used without further purification.

Sample Preparation. *C. thermoaceticum* strain ATCC 39073 was grown with glucose as the carbon source at 55 °C under CO₂ (Ljungdahl & Andreessen, 1978), and cells were harvested as described (Roberts *et al.*, 1992). The C/Fe-SP was purified to homogeneity in an anaerobic chamber (Vacuum Atmospheres) at ~16 °C. Purity after each chromatographic step was determined by SDS–PAGE followed by silver staining (Bio-Rad) and by Western hybridization to polyclonal antibodies (Roberts *et al.*, 1989). For the preparation of the Co(I) sample, a Co(III) enzyme sample was treated with a 4-fold excess of Titanium (III) citrate (Zehnder & Wuhrmann, 1976) and desalted rapidly on a Pensky column (Penefsky, 1977) before freezing in liquid nitrogen. Anaerobic conditions were maintained at all times. EXAFS model compounds were prepared as described previously (Wirt *et al.*, 1992).

Data Collection. Data were collected at the National Synchrotron Light Source, Brookhaven National Laboratory, on beam line X-9B, using a double flat Si(111) crystal monochromator with fixed exit geometry. Harmonics were rejected by a Ni mirror positioned downstream of the monochromator. All experiments were conducted at 115–130 K, and sample temperature was maintained by flowing cooled nitrogen gas through a low-temperature cryostat (Powers *et al.*, 1981). X-ray edge data having 3 eV resolution were collected as described previously (Wirt *et al.*, 1991, 1992). Fifteen EXAFS scans were collected from two different (89 and 76 mg/mL) Co(I) C/Fe-SP samples. To limit radiation damage and minimize X-ray exposure on

the sample, the horizontal beam aperture was reduced (1.8 mm H; 2.0 mm V for EXAFS, 0.5 mm for edge studies), and the position of the beam along the sample was incremented every three scans. Photon flux was 9.40×10^9 photons s^{−1} mm^{−2} at 100 ma beam current (Gmur *et al.*, 1989). Data were generally taken in the range of 100–200 ma. K-α cobalt fluorescence was collected using a 13-element energy resolving germanium detector without dead time corrections. Internal count rates were in the range of 35 000–40 000 counts s^{−1}. For reference signals, mylar tape was mounted at a 45° angle to the X-ray beam to scatter photons counted by a photomultiplier tube positioned perpendicular to the X-ray beam. For an internal standard, cobalt foil calibration spectra were collected simultaneously with each scan using the same collection configuration as the reference signal. This method accounts for shifts in the monochromator.

Data Treatment and Error Analysis. EXAFS data were manipulated and analyzed using a PC-based version of the AT&T Bell Labs EXAFS package on an IBM compatible machine (Scheuring *et al.*, 1994). EXAFS background removal, *k*³ weighting, Fourier filtering, and nonlinear least-squares fitting followed standard procedures (Sagi *et al.*, 1990; Chance *et al.*, 1986; Lee *et al.*, 1981). All scans were examined for edge position and sharp nonstatistical noise glitches prior to data processing. Corrected edge positions were determined by calibrating the edge position of the sample to the edge position of a cobalt foil as described above. Obvious noise glitches were removed prior to further processing. Background subtracted data were Fourier transformed from 1.5 Å^{−1} to 12.5 Å^{−1} in *k*-space using a square window function. To isolate first shell contributions, the Fourier filter window functions were set to 1.0 and 2.0 Å in *r*-space. All data were fit from 4.0 to 11.0 in *k*-space. The data collected for CoTPP was treated in exactly the same manner as that for Co(I) C/Fe-SP.

Errors in the EXAFS analyses were estimated by three methods. To determine the degree of statistical or random noise, partial sums of the total number of scans were independently fit. The differences in fit distances provide an estimate of random noise. Second, systematic errors due to variations in sample preparation, radiation damage, and beam fluctuations are estimated by separate analyses of independently prepared samples. Third, the method of mapping the minimum solution by examination of χ^2 was applied (Lytle *et al.*, 1989). These estimates gave similar errors of ±0.01 Å for distances.

X-ray edge data for the Co(I) C/Fe-SP samples were collected and processed as described in detail previously (Wirt *et al.*, 1991). X-ray edge energy calibrations were obtained by comparison of the x-ray fluorescence and cobalt foil transmission data collected simultaneously. The cobalt edge was assigned as the maximum of the first-derivative fluorescence spectrum and as the minimum of the corresponding first-derivative cobalt foil transmission spectrum. Cobalt edge data were calibrated to the absolute cobalt edge (7709.0 eV). Integrated pre-edge transition intensities (Table 2) are presented as absolute intensities (eV) with the step jump normalized to 1 (Wirt *et al.*, 1991). Errors associated with integrated intensities of pre-edge features were estimated from a combination of statistical noise and errors intrinsic to the method of analysis. Statistical errors varied between 2 and 3% for Co(I) C/Fe-SP samples. Systematic errors inherent to the method of data analysis were calculated by

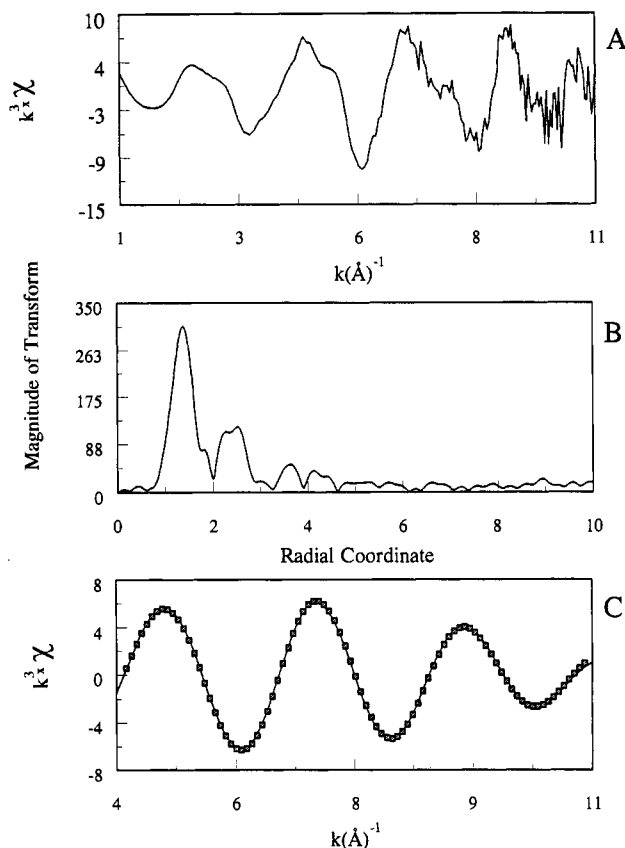


FIGURE 2: (A) Raw data of Co(I) C/Fe-SP in k -space after cubic weighting, background subtraction, and removal of obvious noise glitches. (B) Fourier transform of Co(I) C/Fe-SP data presented in Figure 3A. (C) Back-transformed data from the Co(I) form of the C/Fe-SP after removal of glitches (solid lines) compared with the 1-atom fit simulated solution (D) (squares); $\chi^2 = 0.9$. Data are fit from 4.0 to 11.0 in k -space.

comparison of the integrated peak areas of different scans and from duplicate samples. These systematic errors were $\leq 5\%$. Errors seen in Table 2 represent the error for this measurement taking into consideration both the systematic and statistical errors discussed above.

RESULTS

The XAS data collected on the Co(I) form of the C/Fe-SP, after cubic weighting, background subtraction, and removal of obvious noise glitches, are presented in Figure 2A. Figure 2B shows the Fourier transform of the data shown in Figure 2A. The data were subsequently back-transformed and analyzed using a one-atom fit in which distance (r), Debye–Waller factor shift ($\Delta\sigma^2$), and edge energy shift (ΔE_0) were varied, and the coordination number (N) was held fixed for all solutions except solution D, where it was varied (Table 1). Reported values for $\Delta\sigma^2$ and ΔE_0 were with respect to the model compound. The best fit gave a solution of $r = 1.87 \pm 0.01$ Å, $N = 4.2 \pm 0.3$ ligands, $\Delta\sigma^2 = -2 \times 10^{-4} \pm 0.0006$ Å², $\Delta E_0 = -0.9$ eV, and χ^2 (sum of the residuals squared) = 0.9. Solution D (Table 1) and the experimental data are compared in Figure 2C. A complete series of one-atom fits were conducted by fixing N at various values and examining the effects on χ^2 and the Debye–Waller factors (Table 1). When N was held fixed at 3.0, χ^2 was 20 times greater than that of the well defined minimum with $N = 4.2$. Solutions with coordination numbers greater than four had rapidly increasing values of χ^2 (Table 1). When N was fixed at 5.0, χ^2 was more than seven times that for the minimum solution. Two different two-atom fits were

Table 1: Nonlinear Least-Squares Fitting Solutions for EXAFS Spectra of the Co(I) C/Fe-SP from *C. thermoaceticum*^a

solution	model	r (Å)	N	ΔE_0 (eV)	$\Delta\sigma^2$ (Å ²)	χ^2
A	Co–N	1.86	3.0	–0.5	-3×10^{-3}	22.8
B	Co–N	1.86	3.5	–0.6	-1×10^{-3}	7.9
C	Co–N	1.87	4.0	–0.9	3×10^{-4}	1.6
D	Co–N	1.87	4.2	–0.9	2×10^{-4}	0.9
E	Co–N	1.87	4.5	–0.9	7×10^{-4}	1.6
F	Co–N	1.87	5.0	–1.1	2×10^{-3}	6.5
G	Co–N	1.87	6.0	–1.4	4×10^{-3}	26.3

^a EXAFS solutions (A–G) represent fitting results at various values of fixed coordination number. Parameters: r , distance in Å; N , coordination number; ΔE_0 , energy shift relative to model compound; $\Delta\sigma^2$, Debye–Waller shift relative to model compound; χ^2 , sum of residuals squared. All solutions, except solution D where N was varied, result from fixing N and refining r , σ^2 , and E_0 to minimize χ^2 . EXAFS solutions for Co(I) C/Fe-SP are obtained from Fourier filtered data. The back-transformed data are fit to CoTPP (four nitrogens at 1.949 Å average distance) (Madura *et al.*, 1976) using a nonlinear least-squares fitting procedure.

attempted to examine the possibility of extracting a unique Co–N contribution. Neither a 3(Co–N):1(Co–N) nor a 2(Co–N):2(Co–N) fit gave meaningful solutions. Both series of two-atom fits gave solutions with unreasonable Debye–Waller factors (i.e., values greater than $\pm 1 \times 10^{-2}$ Å²; Chance *et al.*, 1986) that had distance solutions with differences less than the resolution of the data (Lytle *et al.*, 1989). Two-atom fits where the Debye–Waller factors were reasonable contained at least one metal–ligand distance that was not chemically reasonable. Thus, the EXAFS data provides strong evidence that the Co(I) state of the C/Fe-SP adopts a square planar geometry with four N ligands equidistant from the Co nucleus. The C/Fe-SP contains a [4Fe–4S] cluster. There was no evidence of a strong back-scatterer at 3–5 Å (Figure 2B) indicating that the cobalt center and the [4Fe–4S] cluster may be too distant to be observed by the EXAFS technique or that the two metal sites are involved in noncorrelated motion, thereby increasing the Debye–Waller factor and washing out the [4Fe–4S] contribution. Both possibilities are consistent with earlier XAS studies of the Co(II) state of C/Fe-SP (Wirt *et al.*, 1993). Previous ESR (Ragsdale *et al.*, 1987) and redox studies (Harder *et al.*, 1989) of C/Fe-SP have also failed to observe communication between the two metal centers.

Integration of pre-edge features from X-ray edge spectra, followed by comparison of the resulting areas to those for model compounds of known structure, provides a semiquantitative method for predicting coordination number and geometry (Wirt *et al.*, 1991; Bart, 1986; Roe *et al.*, 1984). The edge spectrum of the Co(I) state of the C/Fe-SP (Figure 3) contains a moderate intensity 1s–4p + shake-down transition and no 1s–3d peak, where shake-down (SD) transitions are indicative of transfer of charge from the ligand to the metal in compounds with square-planar geometries (Kosugi *et al.*, 1984; Bair *et al.*, 1980; Kosugi *et al.*, 1986). The presence of the 1s–4p + SD transition and absence of a 1s–3d transition in the edge spectrum of the Co(I)–C/Fe-SP are consistent with a four-coordinate square-planar geometry (Bart, 1986; Roe *et al.*, 1984). Comparison of the integrated 1s–4p + SD transition area for CoTPP, a nearly perfect square-planar complex (Madura *et al.*, 1976; Stevens, 1981), is greater than that for the Co(I) form of the C/Fe-SP (Table 2). A reduction in intensity of the 1s–4p + SD transition, compared with CoTPP, was also observed in the X-ray edge spectrum of the (distorted) square-planar Co(I) B₁₂ interme-

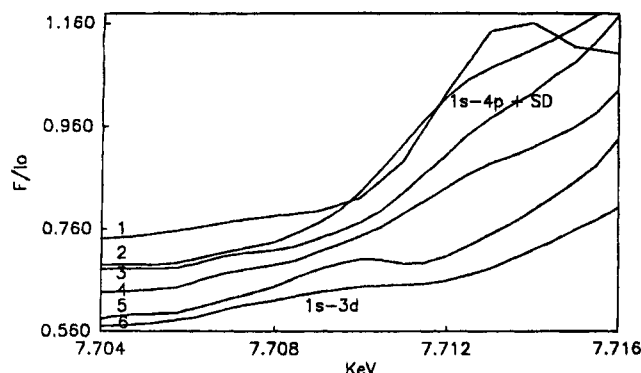


FIGURE 3: X-ray fluorescence pre-edge data of transitions observed in cobalamin models, free cobalamins, and C/Fe-SP compounds. (1) CoTPP, 1s-4p + SD (four-coordinate); (2) Co(I) B₁₂, 1s-4p + SD (four-coordinate); (3) Co(II) C/Fe-SP, 1s-4p + SD (four-coordinate); (4) Co(I) C/Fe-SP, 1s-4p + SD (four-coordinate); (5) Co(II) B₁₂, 1s-3d (five-coordinate); (6) cyanocobalamin, 1s-3d (six-coordinate). X-ray edge spectra are calibrated for energy and intensity comparisons. Spectra have been arbitrarily offset along the Y-axis for comparison.

diate (Wirt *et al.*, 1992) and the four-coordinate Co(II) state of the C/Fe-SP (Wirt *et al.*, 1993a) (Figure 3 and Table 2). This reduction in intensity is likely due to deviation from a pure square-planar geometry since the corrin tetrapyrrole rings A and D are fused (Figure 1). Thus, both our X-ray edge data and EXAFS results provide direct evidence for a four-coordinate (distorted) square-planar configuration for the Co(I) state of the C/Fe-SP.

The first derivatives of the X-ray edge spectra of the various Co(I) species were calculated and compared with that of a cobalt foil, to indicate the effective nuclear charge (ENC) on cobalt. The edge position of the Co(I) state of the C/Fe-SP at 7720.5 ± 0.3 eV was 0.5 eV lower in energy but within the error extremes compared to the value observed for free Co(I) B₁₂ (Table 2). This reduction in ENC for enzyme-bound cofactor was observed for all measured oxidation states, with a 1.0 eV lower ENC for the methyl-Co(III) and Co(II) forms than for base-on Co(III) methylcobalamin and Co(II) B₁₂, respectively. The ENC at cobalt for the five-coordinate methyl-Co(III) state of the C/Fe-SP was 1.5 eV lower than that observed for five-coordinate base-off Co(III) methylcobalamin.

In comparison to the four-coordinate Co(II) state of the C/Fe-SP from *C. thermoaceticum*, the base-off Co(II) state of B₁₂ was found to be quite unstable and could only be observed by photolysis of a base-off methylcobalamin parent species using a time multiplexed laser-photolysis system coupled to a rapid-flow cell (Scheuring *et al.*, 1995) (Figure 4). Rapid generation and observation of the base-off Co(II)

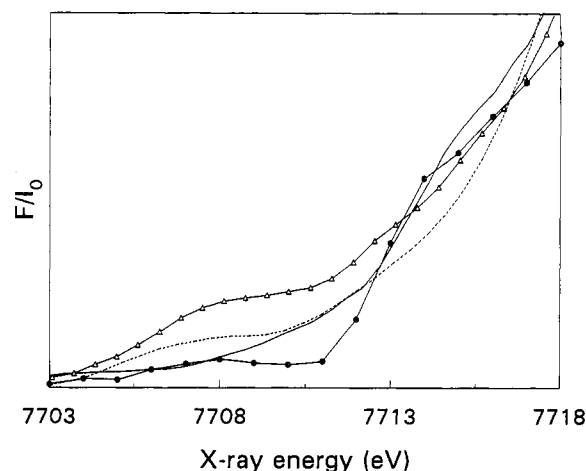


FIGURE 4: X-ray fluorescence pre-edge data (from bottom to top) observed for free base-off Co(II) B₁₂ generated by time-resolved X-ray spectroscopy (solid circles), 1s-4p + SD and 1s-3d observed (the residual 1s-3d transition is due to incomplete conversion of the alkylcobalamin to Co(II), quantum yield = 0.4); Co(II) C/Fe-SP, 1s-4p + SD observed (solid line); free base-off Co(II) B₁₂, generated by chemical reduction stabilized at low temperature, 1s-3d observed (dotted line); free base off methylcobalamin, 1s-3d observed (open triangles). Spectra have been arbitrarily offset along the Y-axis for comparison.

species was required since oxidation to Co(III) occurs quickly at room temperature and coordination of water to the Co(II) species appears to occur at low temperatures. One can observe dramatic differences between the pre-edge features of base-off Co(II) B₁₂ prepared by chemical reduction and immediate quenching in liquid nitrogen, enzyme-bound Co(II) cobinamide, and room temperature Co(II) B₁₂ spectra generated by photolysis (Figure 4). The presence of a moderate intensity 1s-3d transition in the low temperature Co(II) species generated by chemical reduction is consistent with the addition of axial water. Only the enzyme-bound Co(II) cobinamide and free base-off Co(II) B₁₂ generated using time-resolved methods have the 1s-4p + SD transitions characteristic of a four-coordinate structure. For the Co(II) form of C-Fe/SP, we presume the active site excludes solvent while, for the time-resolved photoproduct, the water coordination has not had time to occur (Chen & Chance, 1990).

DISCUSSION

In order for the C/Fe-SP to cycle effectively between the CH₃-Co³⁺ and Co¹⁺ states, there must be mechanisms to prevent homolytic cleavage of the carbon-cobalt bond (which would result in formation of Co²⁺ and an alkyl radical species) and to facilitate reduction of Co²⁺ (which is formed by inadvertent oxidation) to the active Co¹⁺ state. We have observed three characteristics of the C/Fe-SP that may be

Table 2: Integrated X-ray Fluorescence Pre-Edge Transition Intensities and Edge Positions for Co(I), Co(II), and Methyl-Co(III) C/Fe-SP from *C. thermoaceticum*, Free Cobalamins, and Cobalamin Model Compounds

compound	coordination number	1s-3d intensities (eV)	1s-4p + SD intensities (eV)	edge position (eV)
Co(III) hexamine ^a	6	0.020 ± 0.006		7723.5 ± 0.2
Co(II) B _{12a}	5	0.166 ± 0.012		7722.0 ± 0.2
Co(II) TPP ^a	4		1.188 ± 0.006	7721.5 ± 0.2
Co(I) B ₁₂ ^b	4		0.266 ± 0.012	7721.0 ± 0.2
Co(I) C/Fe-SP	4		0.282 ± 0.010	7720.5 ± 0.3
Co(II) C/Fe-SP ^c	4		0.248 ± 0.036	7721.0 ± 0.3
methyl-Co(III) C/Fe-SP ^c (125K)	6	0.256 ± 0.042		7721.5 ± 0.3
Co(III) methylcobalamin ^a	6	0.250 ± 0.016		7722.5 ± 0.2
Co(III) base-off methylcobalamin (180 K) ^d	6	0.316 ± 0.016		7723.0 ± 0.2
Co(III) base-off methylcobalamin (298 K) ^d	5	0.458 ± 0.004		7723.0 ± 0.2

^a Wirt *et al.* (1991). ^b Wirt *et al.* (1992). ^c Wirt *et al.* (1993a). ^d Wirt *et al.* (1993b).

important in minimizing the formation of Co^{2+} : (i) maintenance of base-off coordination geometry, (ii) imposition of a square-planar Co(II) state, and (iii) lowering of the effective nuclear charge on cobalt.

One way that the C/Fe-SP appears to facilitate reduction of oxidatively produced inactive Co^{2+} and protect against homolysis of the methyl- Co^{3+} bond is by control of the ligation state of the cobalt center. In all three redox states, the benzimidazole group remains uncoordinated to cobalt. It was shown earlier that removal of the benzimidazole base as an axial ligand could account for the increased stability of Co^{1+} (by ~ 12 kJ/mol) in the C/Fe-SP (Harder *et al.*, 1989). The Co III/II and Co(II)/(I) reduction potentials were found to be ~ 100 mV more positive for the enzyme-bound cobamide than that found for free cobalamin (Harder *et al.*, 1989). Maintenance of the base-off conformation is also thought to protect methyl- Co(III) species from a homolytic cleavage event that would disadvantageously form a methyl radical and inactive Co(II) state of the C/Fe-SP (Martin *et al.*, 1992). Not only is the Co^{2+} state base off in the C/Fe-SP, but it also adopts an unusual four-coordinate planar geometry (Wirt *et al.*, 1993). As shown here, the same geometry is observed for Co^{1+} in C/Fe-SP similar to that previously observed for free Co(I) B_{12} (Wirt *et al.*, 1992). Imposition of the Co^{1+} geometry on the Co^{2+} state would be expected to enhance the rate of reduction of Co^{2+} since there would be no requirement for accompanying reorganization of the ligand sphere.

There are examples of protein-bound cobamides which have $\text{Co}^{2+/1+}$ redox potentials in the same range as observed for the C/Fe-SP and which have a coordinated aromatic nitrogen donor ligand (Banerjee *et al.*, 1990). Therefore, one wonders if other effects may play a role in controlling the reactivity of cobamide and alkyl cobamide for the C/Fe-SP.

A third characteristic of all these states of the cobamide is the lowered effective nuclear charge on cobalt relative to B_{12} in solution. For methyl Co^{3+} , Co^{2+} , and Co^{1+} , the ENC is lowered by 1–1.5, 1.0, and 0.5 eV relative to B_{12} in solution (for the latter this is within the error range). The mechanistic implication of this may include the following. To maintain neutral charge on $\text{CH}_3\text{-Co}^{3+}$, it is likely that electron density has been transferred from the protein, corrin ring, or methyl group to the cobalt center. In free methylcobalamin this effect is observed as a reduction in ENC relative to non- σ -bonding axial ligands [cf., Table 1 and Wirt *et al.*, (1991)]. In the enzyme case, the methyl group may become even more electrophilic, facilitating the nucleophilic attack by a methyl group acceptor on the CODH forming the methyl-CODH product. Similarly, for the Co^{1+} state of the C/Fe-SP, transfer of electron density to lower the charge on Co would increase its ability to displace the methyl group of $\text{CH}_3\text{-H}_2$ folate. In any case, the C/Fe-SP enzyme provides unique electronic and structural influences on the cobamide cofactor that are entirely consistent with the known mechanism.

ACKNOWLEDGMENT

We thank Yang Hai and Mike Sullivan for technical assistance at beamline X-9B. The construction and operation of beamline X-9B is supported by National Institute of Health Grant P-41-RR-01633. The National Synchrotron Light Source, Brookhaven National Laboratory, is supported by the Department of Energy, Division of Materials Sciences

and Division of Chemical Sciences (DOE Contract No. DE-AC02-76CH00016). Chem-X molecular modeling programs are developed and distributed by Chemical Design Ltd., Oxford, England.

REFERENCES

- Allen, F. H., Kennard, O., & Taylor, R. (1983) *Acc. Chem. Res.* 16, 146–153.
- Bair, R. A., & Goddard, W. A. (1980) *Phys. Rev. B* 22, 2767–2776.
- Banerjee, R. V., Harder, S. R., Ragsdale, S. W., & Matthews, R. G. (1990) *Biochemistry* 29, 1129–1135.
- Bart, C. (1986) *Advances in Catalysis* (Eley, D. D., Pines, H., & Weisz, P. B., Eds.) Vol. 34, pp 203–296, Academic Press, Orlando, FL.
- Chance, M. R., Powers, L. S., Kumar, C., & Chance, B. (1986) *Biochemistry* 25, 1259–1265.
- Chen, E., & Chance, M. R. (1990) *J. Biol. Chem.* 265, 12987–12994.
- Gmur, N. F., Thomlinson, W., & White-DePace, S. (1989) *National Synchrotron Light Source User's Manual: Guide to the VUV and X-Ray Beamlines*, 3rd ed., BNL 42276 Informal Report, National Technical Information Service, X9A.
- Harder, S. R., Lu, W. P., Feinberg, B. A., & Ragsdale, S. W. (1989) *Biochemistry* 28, 9080–9087.
- Hu, S.-I., Pezacka, E., & Wood, H. G. (1984) *J. Biol. Chem.* 259, 8892–8897.
- Kosugi, N., Yokoyama, T., Asakura, K., & Kuroda, H. (1984) *Chem. Phys.* 91, 249–256.
- Kosugi, N., Yokoyama, T., & Kuroda, H. (1986) *Chem. Phys.* 104, 449–453.
- Krautler, B. (1987) *Helv. Chim. Acta* 70, 1268.
- Lee, P., Citrin, P., Eisenberger, P., & Kincaid, B. (1981) *Rev. Mod. Phys.* 53, 769–806.
- Ljungdahl, L. G., & Andreessen, J. R. (1978) *Methods Enzymol.* 53, 360–372.
- Lu, W.-P., Harder, S. R., & Ragsdale, S. W. (1990) *J. Biol. Chem.* 265, 3124–3133.
- Lytle, F., Sayers, W. D. E., & Stern, E. A. (1989) *Physica B* 158, 701–722.
- Madura, P., & Scheidt, W. R. (1976) *Inorg. Chem.* 15, 3182–3184.
- Martin, B. D., & Finke, R. G. (1992) *J. Am. Chem. Soc.* 114, 585–592.
- Penefsky, H. S. (1977) *J. Biol. Chem.* 252, 2891–2899.
- Powers, L. S., Chance, B., Ching, Y., & Angiolillo, P. (1981) *Biophys. J.* 34, 465–498.
- Ragsdale, S. W., Lindahl, P. A., & Munck, E. (1987) *J. Biol. Chem.* 262, 14289–14297.
- Roberts, D. L., James-Hagstrom, J. E., Garvin, D. K., Gorst, C. M., Runquist, J. A., Baur, J. R., Haase, F. C., & Ragsdale, S. W. (1989) *Proc. Natl. Acad. Sci. U.S.A.* 86, 32–36.
- Roberts, J. R., Lu, L.-P., & Ragsdale, S. W. (1992) *J. Bacteriol.* 174, 4667–4676.
- Roe, A. L., Schneider, D. J., Mayer, R. J., Pyrz, J. W., Widom, J., & Que, L. (1984) *J. Am. Chem. Soc.* 106, 1676–1681.
- Rossi, M., Glusker, J. P., Randaccio, L., Summers, M. F., Toscano, P. J., & Marzilli, L. G. (1985) *J. Am. Chem. Soc.* 107, 1729–1738.
- Sagi, I., Wirt, M. D., Chen, E., Frisbie, S. M., & Chance, M. R. (1990) *J. Am. Chem. Soc.* 112, 8639–8644.
- Scheuring, E. M., Sagi, I., & Chance, M. R. (1994) *Biochemistry* 33, 6310–6315.
- Scheuring, E. M., Clavin, W., Wirt, M. W., Miller, L. M., Lu, Y., Mahoney, N., Xie, A., Wu, J.-J., & Chance, M. R. (1995) *J. Phys. Chem.* (submitted).
- Stevens, E. J. (1981) *J. Am. Chem. Soc.* 103, 5087–5095.
- Wirt, M. D., & Chance, M. R. (1993) *J. Inorg. Biochem.* 49, 265–273.
- Wirt, M. D., Sagi, I., Chen, E., Frisbie, S. M., Lee, R., & Chance, M. R. (1991) *J. Am. Chem. Soc.* 113, 5299–5304.
- Wirt, M. D., Sagi, I., & Chance, M. R. (1992) *Biophysical J.* 63, 412–417.
- Wirt, M. D., Kumar, M., Ragsdale, S. W., & Chance, M. R. (1993) *J. Am. Chem. Soc.* 115, 2146–2150.
- Zehnder, A. J. B., & Wuhrmann, K. (1976) *Science* 194, 1165–1166.